General Disclaimer

One or more of the Following Statements may affect this Document

- This document has been reproduced from the best copy furnished by the organizational source. It is being released in the interest of making available as much information as possible.

- This document may contain data, which exceeds the sheet parameters. It was furnished in this condition by the organizational source and is the best copy available.

- This document may contain tone-on-tone or color graphs, charts and/or pictures, which have been reproduced in black and white.

- This document is paginated as submitted by the original source.

- Portions of this document are not fully legible due to the historical nature of some of the material. However, it is the best reproduction available from the original submission.

Produced by the NASA Center for Aerospace Information (CASI)

NASA Contractor Report 174871

Application of Homomorphic Signal Processing to Stress Wave Factor Analysis

Hira Karagulle, James H. Williams, Jr., and Samson S. Lee

Massachusetts Institute of Technology
Cambridge, Massachusetts

APPLICATION OF HOMOMORPHIC SIGNAL PROCESSING TO STRESS WAVE FACTOR ANALYSIS
(Massachusetts Inst. of Tech.) 48 p
HC A03/MF A01
CSCL 14D
G3/38
N85-21673
Unclas
14424

February 1985

Prepared for

NATIONAL AERONAUTICS AND SPACE ADMINISTRATION
Lewis Research Center
Under Grant NSG 3-328

ABSTRACT

The stress wave factor (SWF) signal, which is the output of an ultrasonic testing system where the transmitting and receiving transducers are coupled to the same face of the test structure, is analyzed in the frequency domain. The SWF signal generated in an isotropic elastic plate is modelled as the superposition of successive reflections. The reflection which is generated by the stress waves which travel p times as a longitudinal (P) wave and s times as a shear (S) wave through the plate while reflecting back and forth between the bottom and top faces of the plate is designated as the reflection with p, s. Short- time portions of the SWF signal are considered for obtaining spectral information on individual reflections. If the significant reflections are not overlapped, the short- time Fourier analysis is used.

A summary of the relevant points of homomorphic signal processing, which is also called cepstrum analysis, is given. Homomorphic signal processing is applied to short- time SWF signals to obtain estimates of the log spectra of individual reflections for cases in which the reflections are overlapped.

Two typical SWF signals generated in aluminum plates are analyzed. In Test I, the SWF signal contains nonoverlapping reflections. In Test II, the thickness of the plate is approximately half that in Test I, and the reflections are overlapped. Multiple reflections of only P waves are considered. It is observed that the log spectra of two corresponding reflections with the same ray angles and approxiamtely the same total ray path lengths in Tests I and II have approximately the same characteristics except for their overall scales, as the theory of wave propagation in isotropic elastic plates suggests. From the differences between the overall scales and

the values of p of the two corresponding reflections in Tests I and II, experimental reflection coefficients for P wave to P wave reflections are obtained for the different ray angles considered. They show good agreement with the theoretical reflection coefficients for plane P waves. Also, it is observed that the frequency response at the maximum value of the log spectrum moves toward higher frequencies in the reflections with larger p, namely with smaller ray angles. This is consistent with the behavior of the directivity function.

The potential use of these results for the nondestructive evaluation of plates containing cracks perpendicular to their faces is demonstrated in a specific test.

1 INTRODUCTION

The measurements of nondestructive evaluation (NDE) parameters in an ultrasonic testing (UT) system may be conducted directly on the input and output signals or indirectly on a processed signal [1]. These indirect techniques usually take the form of a transformation of a signal into another signal on which the interpretations of the measurements for NDE may be easier.The Fourier transform is one of the most commonly used signal processing analytical tools.

Recently, UT systems in general have the input and output signals in the form of discrete- time signals (sequences) and they are processed on a digital computer. This is faciliated by the availability of high frequency analog to digital converters, and the efficient algorithm for computation of the Fourier transform known as the fast Fourier transform (FFT) [2]. There are increasingly sophisticated signal processing algorithms developed to exploit the flexibility of the digital computer [3]. Ultrasonic NDE applications of these algorithms are current research areas. An example of a class of algorithms of this type is the set of techniques referred to as cepstrum analysis or homomorphic signal processing [3], which is used in this study.

In general, a pulse having a broadband frequency spectrum or a tone burst is used as the input signal in a UT system. The output signal may consist of superposed pulses or tone bursts,respectively, which arise due to reflections from the boundaries of the test structure. In conventional UT techniques [4] such as the pulse- echo or through- thickness transmission methods, the measurements are conducted directly in the time domain. Peak values of pulses or magnitudes of tone bursts and their time delays are

measured. These methods are limited to output signals which contain nonoverlapping pulses or tone bursts.

In conventional ultrasonic spectral techniques [5], measurements on the output signal are conducted in the frequency domain. The magnitude or phase spectra of the individual pulses are analyzed. These methods are also limited to output signals with nonoverlapping pulses.

Recently [illegible]ry et al. [6,7] introduced an ultrasonic NDE parameter called the "stress wave factor" (SWF). Separate transmitting and receiving transducers are coupled to the same face of the test structure, which is called the SWF configuration. An input pulse having a broadband frequency spectrum is applied to the transmitting transducer and the number of oscillations in the output signal at the receiving transducer exceeding a preselected voltage threshold (or some modifications thereof [8]) is defined as the SWF. The SWF is also valid for the analysis of the output signals with overlapping echoes.

The SWF analysis has shown encouraging results in several NDE applications [6-9], and its use in new applications is currently under study [9]. This work is part of an overall effort to develop quantitative analyses of the SWF and computer- aided nondestructive evaluation (CANDE) capabilities. The stress wave transmission chracteristics of an isotropic elastic plate through which the transmitting and receiving transducers communicate in the SWF configuration are studied in [10] and [11]. The SWF signal is modelled as the superposition of the signals due to the stress waves which multiply reflect between the top and bottom faces of the plate. The experimental system used in this study is characterized in [12]. The purpose of this study is the spectral analysis of the SWF signal where the multiple reflections may be

overlapped. Homomorphic signal processing techniques are applied to extract information about the magnitude spectrum of an individual reflection. The measurements on the magnitude spectra of individual reflections may be easily quantifiably examined for NDE applications. The results of this study should provide more efficient and revealing CANDE schemes utilizing the SWF and advanced digital signal processing techniques.

Although the SWF has been generally used to characterize microstructural defect states of materials, it may also be used to detect cracks and delaminations. The output in the SWF configuration may be significantly affected by cracks oriented perpendicular to the faces of the test structure, which might be otherwise difficult to detect by many NDE methods.

2 SWF OUTPUT SIGNAL

Steady- state harmonic stress wave transmission characteristics of an isotropic elastic plate with the transmitting and receiving transducers in the SWF configuration are analyzed in [10] and [11]. Circular transmitting and receiving transducers are considered. It is assumed that the transmitting transducer transforms an electrical voltage into a uniform normal stress at the top face of the plate. Ignoring the bottom boundary, the radiation into a half space is considered first. This introduces longitudinal (P) and shear (S) waves into the plate. Then the reflections which introduce reflected P and S waves for each incident P or S wave are considered successively at the bottom and top faces of the plate. For example, the multiply reflected wave specified by the chain PPSP is constructed from the half space solution as a P wave which reflects as a P wave at the bottom face, then as an S wave at the top face, and again as a P wave at the bottom face. The total number of P's and S's in the chain is denoted by p and s, respectively. It is assumed that the receiving transducer produces an electrical voltage proportional to the average spatially integrated normal stress over the face of the transducer due to an incident wave. The exact solution for the frequency response of the plate is formulated in integral form as the superposition of the frequency responses due to all the possible multiply reflected waves which reflect at the bottom face a final time and are then incident upon the receiving transducer. It is found that the phases of the frequency responses due to the waves with common p and s have the same linear dependence on frequency. Thus the waves with common p and s; simply the waves with p,s; have the same time delays in the transient analysis. For example the waves with p=3,s=1 are the

the waves specified by the chains PPPS, PPSP, PSPP, and SPPP.

The asymptotic behavior of the frequency response due to a multiply reflected wave is also analysed. It is found that a receiving point observes an incident wave asymptotically as a plane wave which propagates and reflects in the direction of the multiply reflected ray constructed geometrically using Snell's law. The far field condition for the asymptotic solution to be valid is discussed. It suggests that although the thickness of the plate may be small, waves which have a sufficiently large total ray path length will satisfy the far field condition. Formulae for the time delays for waves travelling the ray path length are also given.

The analysis given in [10] and [11] then suggests that the SWF signal can be modelled as the superposition of multiple reflections given by

$$y(n) = \sum_{p+s=2,\,s=0}^{p+s=\infty,\,s=\infty} y_{p,s}(n-n_{p,s}) \qquad (1)$$

where $p+s=2,4,6,\ldots$ and $s=0,1,2,\ldots$. Further, $y(n)$ is the discrete- time SWF signal, $y_{p,s}(n-n_{p,s})$ is the sample sequence of the reflection generated by the waves with p,s; or stated otherwise, simply the reflection with p,s. n is an integer which defines the discrete- time location t by

$$t = n\,T \qquad (2)$$

where T is the sampling period. The reciprocal of T is called the sampling frequency. $n_{p,s}$ is the delay for the reflection with p,s. Only even values of p+s are considered in eqn. (1) because the corresponding waves satisfy the

condition that they reflect at the bottom face last time.

It is assumed that the test specimen and all the components of the experimental system are linear and time invariant. Then, the following can be written [3]

$$y_{p,s}(n-n_{p,s}) = x(n) * h_e(n) * h_{p,s}(n-n_{p,s}) \qquad (3)$$

where * denotes the linear convolution operation [3]. $x(n)$ is the input signal which generates the SWF signal. $h_e(n)$ is the sample sequence of the impulse response of the experimental system without a test specimen. $h_{p,s}(n-n_{p,s})$ is the sample sequence of the impulse response due to the waves with p,s. As discussed above, the continuous frequency response due to a multiply reflected wave in the plate is studied in [10] and [11]. Assuming that the sampling frequency is greater than the Nyquist frequency, the FFT of $h_{p,s}(n-n_{p,s})$ is the sample sequence of the continuous frequency response due to the waves with p,s scaled by 1/T [3,12].

3 HOMOMORPHIC PROCESSING OF SWF SIGNAL

If there exists a signal that is the sum of two component signals whose Fourier transforms occupy different frequency bands, then it is possible to separate the two components by a linear filter. On the other hand if there exists a signal that is the multiplication or convolution of two component signals, then it may be possible to separate the two components by a homomorphic filter [3].

Below, the properties of a short- time portion of a SWF signal, which is called the short- time SWF signal, are discussed first. Then, the properties of homomorphic systems are summarized and homomorphic signal processing is applied to the short- time SWF signal to obtain estimates of the magnitude spectra of individual reflections despite the fact that the successive reflections may be overlapped.

3.1 Short-Time SWF Signal

For the purpose of the analysis in this study, the complete SWF signal is multiplied by a window w(n) which gives the short- time SWF signal $y_w(n)$ as

$$y_w(n) = w(n)\ y(n) \qquad (4)$$

where w(n) is called the data window.

If the significant reflections in the SWF signal are not overlapped, a rectangular data window is used and its time interval is chosen such that the short- time SWF signal contains only an individual reflection and excludes all

the other reflections completely. Then, by taking the FFT of short- time SWF signals, the magnitude spectra of individual reflections can be found directly as in conventional ultrasonic spectral techniques [5]. This is also called the short- time Fourier analysis [13].

If the reflections in the SWF signal are overlapped, it is no longer possible to obtain spectral information on individual reflections directly by the short- time Fourier analysis. However, it may be possible to obtain estimates of the magnitude spectra of individual reflections by the short- time homomorphic analysis. For this purpose the short- time SWF signal must be defined appropriately as described below.

First, it is assumed that the reflections whose delays are inside the data window are completely covered by $y_w(n)$, otherwise they are completely outside the window. It is impossible to satisfy this condition exactly when the reflections are overlapped. However it may be satisfied approximately by using a data window which is long enough and tapered smoothly to zero at the beginning and the end. Standard Hamming, Hanning, or Blackman windows [3] may be appropriate for this purpose. Then using eqns. (1) and (4)

$$y_w(n) \approx w(n) \sum_{j=1}^{J} y_j(n-n_j) \qquad (5)$$

where the index j replaces the complex index (p,s) in eqn. (1) such that $n_j=n_{p,s}$ and $n_1<n_2<n_3<\ldots<n_J$. In this notation, the reflections in the data window are ordered according to their delays. J is the total number of reflections in the window. $y_j(n-n_j)$ is equal to $y_{p,s}(n-n_{p,s})$ accordingly.

Second, it is assumed that the individual reflections in the window have

approximately the same waveform but they differ only by a scale. Suppose the scale of the reflection $y_m(n-n_m)$ is maximum compared with the scales of the other reflections in the window and that it is unity. Then the other reflections can be written as

$$y_j(n-n_j) \approx A_j\, y_m(n-n_j) \qquad (6)$$

where A_j is the scale of the reflection having the delay n_j and it is smaller than or equal to unity, given that A_m is equal to unity.

The asymptotic ray analysis in [10] and [11] suggests that each reflection is generated by the stress waves in the plate which propagate and reflect in a particular multiply reflected ray direction, which is constructed geometrically via Snell's law. The direction is defined by the ray angle; that is, the angle between the ray and the transmitting transducer axis. The frequency components of the input signal are transmitted in the ray directions according to the directivity functions which are given and discussed in detail in [10] and [11].

For the P waves, the increasingly higher frequency components are transmitted at decreasing ray angles. The individual reflections with larger numbers of p, namely with larger delays, have smaller ray angles. Thus, for P waves, the reflections with larger delays tend to contain higher frequency components. So, the spectral contents of two reflections may differ significantly if the difference between their ray angles is large; namely, the difference between their delays is large. Thus, these two hypothetical reflections also differ in the time domain significantly. The condition in eqn. (6) is then satisfied better when the length of the data window is not

very long. Also, using a window which is tapered smoothly to zero at the beginning and the end decreases the contribution of the reflections at the beginning and end of the short- time SWF signal.

So, the conditions given in eqns. (5) and (6) both are satisfied better when the data window is tapered smoothly to zero at the beginning and the and. However, eqn. (5) requires a longer window, whereas eqn. (6) requires a shorter one. Thus, there is a compromise in the length of the data window.

Substituting eqn. (6) into eqn. (5)

$$v_w(n) \approx w(n) \sum_{j=1}^{J} A_j \, y_m(n-n_j) \tag{7}$$

Eqn. (7) can also be written as

$$y_w(n) \approx w(n) \, [y_m(n) * p(n)] \tag{8}$$

where

$$p(n) = \sum_{j=1}^{J} A_j \, \delta(n-n_j) \tag{9}$$

and

$$\delta(n-n_j) = \begin{cases} 1 & , \quad n=n_j \\ 0 & , \quad n \neq n_j \end{cases} \tag{10}$$

where $\delta(n)$ is called the impulse sequence and $p(n)$ is called an impulse train.

An impulse train is defined as a sequence in which the nonzero samples are spaced at intervals that are greater than one [14].

Assuming that w(n) varies slowly with respect to $y_m(n)$, eqn. (8) can be written as [3,13]

$$y_w(n) \approx p_w(n) * y_m(n) \tag{11}$$

where

$$p_w(n) = w(n)\ p(n) \tag{12}$$

Using eqns. (9),(10) and (12),

$$p_w(n) = \sum_{j=1}^{J} B_j\ \delta(n-n_j) \tag{13}$$

where

$$B_j = A_j\ w(n_j) \tag{14}$$

It is assumed that the data window is located such that

$$B_m = w(n_m) \approx 1 \tag{15}$$

Eqn. (15) is satisfied when the middle of the window is located near the delay n_m in the case of Hamming, Hanning, or Blackman windows [3].

By taking the FFT of the short- time SWF signal $y_w(n)$, eqn. (11) becomes

$$Y_w(k) \approx P_w(k)\ Y_m(k) \qquad (16)$$

where $Y_w(k)$, $P_w(k)$, and $Y_m(k)$ are the FFT's of $y_w(n)$, $p_w(n)$, and $y_m(n)$, respectively. k is an integer and defines the discrete- frequency location f by

$$f = \frac{k}{N_f}\ \frac{1}{T} \qquad (17)$$

where N_f is the number of points for the FFT operation, which is some power of two. It is assumed that N_f is adequately large so that the multiplication in eqn. (16) corresponds to the linear convolution in eqn. (11), the conditions for which are discussed in [3] and [12].

By taking the magnitude of $Y_w(k)$, eqn. (16) becomes

$$|Y_w(k)| \approx |P_w(k)|\ |Y_m(k)| \qquad (18)$$

where | | denotes the "magnitude of".

So, the magnitude spectrum of the short- time SWF signal $|Y_w(k)|$ is approximately equal to the multiplication of two component magnitude spectra, namely, the magnitude spectrum of an impulse train $|P_w(k)|$ and the magnitude spectrum of the particular reflection with the delay n_m $|Y_m(k)|$. Below, $|Y_m(k)|$ is obtained from $|Y_w(k)|$ by homomorphic signal processing.

3.2 Homomorphic Signal Processing

A detailed discussion of homomorphic signal processing is given in [5] and [13]. Only a summary of the relevant points is pr vided here.

Suppose H denotes the transformation of a system such that

$$z(n) = H[s(n)] \tag{19}$$

where s(n) and z(n) are the input and output of the system, respectively. Suppose that H satisfies the generalized principle of superposition under some rules of combinations (for example, addition, multiplication, convolution) in the inputs and outputs as

$$\begin{aligned} H[s_1(n) \,\square\, s_2(n)] &= H[s_1(n)] \circ H[s_2(n)] \\ &= z_1(n) \circ z_2(n) \end{aligned} \tag{20}$$

where $s_1(n)$ and $s_2(n)$ are two arbitrary signals. The symbols $\square$ and $\circ$ designate the rules for combining the inputs and outputs, respectively, and they are both commutative and associative [3]. The symbols $\square$ and $\circ$ are also called the input and output operations, respectively. The class of systems satisfying the generalized principle of superposition is called homomorphic systems [15]. Linear systems are a special case for which the input and output operations are both addition.

Any homomorphic system can be decomposed into three cascaded systems via the ordered transformations $D_{\square}$, L, and $D_{\circ}^{-1}$ [3,15]. For the system H, the system $D_{\square}$ is a homomorphic system and has the property that

$$D_{\square}[s_1(n) \square s_2(n)] = D_{\square}[s_1(n)] + D_{\square}[s_2(n)]$$
$$= s_1(n) + s_2(n) \qquad (21)$$

As observed in eqn. (21) the system $D_{\square}$ transforms the combinations according to the rule $\square$ to the additive combinations.

The system L is a linear system and has the property that

$$L[s_1(n) + s_2(n)] = L[s_1(n)] + L[s_2(n)]$$
$$= \tilde{q}_1(n) + \tilde{q}_2(n) \qquad (22)$$

The system D_o^{-1} is a homomorphic system and it has the property that

$$D_o^{-1}[\tilde{q}_1(n) + \tilde{q}_2(n)] = D_o^{-1}[\tilde{q}_1(n)] \circ D_o^{-1}[\tilde{q}_2(n)]$$
$$= z_1(n) \circ z_2(n) \qquad (23)$$

As observed in eqn. (23) D_o^{-1} transforms the additive combinations to the combinations according to the rule o.

If there is a signal that is the combination of two component signals under the rule $\square$, then it may be possible to separate the two components by a homomorphic filter whose input and output operations are both $\square$. This essentially reduces to the problem of designing the linear system L [3].

Homomorphic signal processing has been successfully applied to the analysis of audio signals [16], images [16], speech signals [16,17,18,19], seismic signals [20], and echo removal [14]. In this study it is applied to the analysis of the SWF signal.

The schematic of the homomorphic signal processing applied to the SWF output signal to estimate the magnitude spectrum of a particular reflection is shown in Fig. 1. The operations applied to the SWF signal in Sec. 3.1 are also included in Fig. 1. The magnitude spectrum of the short- time SWF signal $|Y_w(k)|$ is the input to the homomorphic system. Since $|Y_w(k)|$ is the multiplication of two components $|P_w(k)|$ and $|Y_m(k)|$ as given in eqn. (18), the input and output operations of the homomorphic system are both multiplication. Then, the corresponding systems $D_{\square}$ and $D_{\circ}$ are designated as $D_{\cdot}$ and $D_{\cdot}^{-1}$, respectively, where the subscript $\cdot$ denotes the multiplication operation. The suitable systems $D_{\cdot}$, L, and $D_{\cdot}^{-1}$ satisfying the conditions in eqns. (19), (20), and (21), respectively, are indicated in Fig. 1.

If the logarithm of both sides of eqn. (18) is taken

$$\log|Y_w(k)| \approx \log|P_w(k)| + \log|Y_m(k)| \qquad (24)$$

The logarithmic magnitude spectrum (log spectrum) of an impulse train is rapidly varying. If the impulses are equally spaced then it is periodic [21]. It is assumed that the log spectrum of the reflection with the delay n_m, $\log|Y_m(k)|$, is slowly varying compared with the log spectrum of the impulse train, $\log|P_w(k)|$. Then it is possible to separate these two superposed components by linear filtering [3]. Since the filtering is done on a spectrum, it is called frequency- invariant linear filtering and it is exactly parallel to the usual low- pass or high- pass time- invariant linear filtering which extracts either the respective slowly varying or the rapidly varying component of a signal in the time domain [3].

The suitable frequency- invariant linear filtering is performed first by

taking the inverse fast Fourier transform (IFFT) of $\log|Y_w(k)|$. The IFFT of the log spectrum is called the cepstrum [3], a term first introduced in [22]. So, eqn. (24) becomes

$$\tilde{y}_w(n) \approx \tilde{p}_w(n) + \tilde{y}_m(n) \qquad (25)$$

where $\tilde{y}_w(n)$, $\tilde{p}_w(n)$, and $\tilde{y}_m(n)$ are the IFFT's of $\log|Y_w(k)|$, $\log|P_w(k)|$, and $\log|Y_m(k)|$, respectively; or the cepstrums of $y_w(n)$, $p_w(n)$, and $y_m(n)$, respectively.

Since $\log|Y_w(k)|$ is slowly varying and $\log|P_w(k)|$ is rapidly varying, their IFFT's $\tilde{y}_m(n)$ and $\tilde{p}_w(n)$ occupy the low- time and high- time portions of the cepstrum $\tilde{y}_w(n)$, respectively. Thus, the cepstrum of $y_m(n)$ may be recovered from the cepstrum of $\tilde{y}_w(n)$ as

$$\tilde{y}_m(n) \approx \tilde{w}_c(n)\ \tilde{y}_w(n) \qquad (26)$$

where $\tilde{w}_c(n)$ is called the cepstrum window and covers the low- time portion of $\tilde{y}_w(n)$.

The properties of the cepstrum are discussed in [3]. In particular it is symmetric about zero. The cepstrum of a signal similar to $y_m(n)$, which has a slowly varying log spectrum, is concentrated near zero time and decays rapidly away from zero. Specifically, if $y_m(n)$ is N_y samples long, then its cepstrum $\tilde{y}_m(n)$ occupies mainly the interval approximately from $-N_y/3$ to $N_y/3$ [20]. Thus, the cepstrum window is chosen such that it covers this interval.

The cepstrum of an impulse train is discussed in [3], [13], and [20]. If the impulse train is equally spaced with a spacing interval N_p, then its

cepstrum shows peaks at the locations of jN_p where $j=\pm(1,2,3,\ldots)$, which reflects the periodicity of the log spectrum of the impulse train. So, $\tilde{y}_m(n)$ and $\tilde{p}_w(n)$ are well seperated in $\tilde{y}_w(n)$ when N_p is greater than $N_y/3$, which limits the validity of eqn. (26).

If the impulses are located arbitrarily and they have amplitudes of arbitrary strength and random polarity, the impulse train may be thought of as a noiselike random signal. Then its log spectrum is rapidly varying but not periodic. Thus its cepstrum does not show any peaks. However, eqn. (26) may be still valid [3,13].

Once $\tilde{y}_m(n)$ is recovered by eqn. (26), $\log|Y_m(k)|$ is found by taking the FFT of $\tilde{y}_m(n)$, and then $|Y_m(k)|$ is found by exponentiation of $\log|Y_m(k)|$. $\log|Y_m(k)|$, which is the log spectrum of the reflection $y_m(n)$, is also called the cepstrally smoothed log spectrum of the short- time SWF signal $y_w(n)$.

The time history of the reflection $y_m(n)$ cannot be found by the process shown in Fig. 1 because the logarithm operation is performed on $|Y_w(k)|$ and the phase information is lost. If the complex logarithm operation is performed on $Y_w(k)$ then it may be possible to find $y_m(n)$ by adding another IFFT operation to the end of the process. The complex logarithm requires unwrapping of the phase of $Y_w(k)$ to obtain a continuous phase curve [3]. The corresponding term for the cepstrum is called the complex cepstrum, which is the IFFT of the complex logarithm of the FFT of a time domain signal. For the analysis in this study, the cepstrum is used rather than the complex cepstrum.

4 RESULTS AND DISCUSSIONS

The experimental system used in this study is characterized in [12] by coupling the transmitting and receiving transducers face- to- face, without a test specimen in between. The impulse response of the experimental system and its log spectrum are shown in Figs. 2 (a) and 2 (b), respectively. The signal in Fig. 2 (a) and all the time domain signals in the subsequent figures are discrete; their sampling period is 0.05 μsec (sampling frequency 20 MHz). The log spectrum in Fig. 2(b) and all the fraquency domain plots in the subsequent figures are also discrete. They are generated by a 512-point FFT. The points in all the time and frequency domain plots are connected by linear interpolation.

The time history of the input signal to generate the following SWF signals, and its log spectrum are shown in Figs. 3 (a) and 3 (b), respectively. Two tests are considered as typical examples for the SWF signal. In Test I, the thickness of the plate h is 2.4 cm and the distance between the transmitting and receiving transducer axes ℓ is 6 cm. In Test II, h is 1.25 cm and ℓ is 6.25 cm. The plates are made of aluminum (6061-T6), which has P wave and S wave velocites of 0.632 and 0.313 cm/μsec, respectively. The transducers (Panametrics model V105) have a radius of 1.125 cm. The SWF signals for Tests I and II are shown in Figs. 4 (a) and 4 (b), respectively. The time delays for some possible reflections are calculated by the formulae given in [11] considering the multiply reflected rays connecting the centers of the transducers, and their locations are indicated above the time signals with the values of p and s.

The ray angles, total ray path lengths, and time delays for some

reflections with only P waves (s=0) in Tests I and II are given in Table 1. These are calculated using the formulae given in [10] and [11]. The distances between the transducer axes are chosen such that the ray angle for a reflection with $p=p_1$, $s=0$ in Test I is the same as the ray angle for the reflection with $p=2p_1$, $s=0$ in Test II, where p_1 is an arbitrary positive even integer. As observed from Table 1 for some selected values of p_1, their total ray path lengths and time delays are also approximately the same. Then, it is expected from the analysis in [10] and [11] that these two corresponding reflections have the same waveform because all the frequency components of the input signal are transmitted to the receiving transducer in the same direction as discussed in Sec. 3.

The reflection with $p=p_1$, $s=0$ in Test I and the reflection with $p=2p_1$, $s=0$ in Test II are generated from the stress waves which reflect successively at the bottom and top faces of the plate (p_1-1) and $(2p_1-1)$ times, respectively. Thus, it is also expected that the reflection with $p=2p_1$, $s=0$ in Test II is approximately $(Q_{PP})^P$ times smaller than the reflection with $p=p_1$, $s=0$ in Test I, where Q_{PP} is the reflection coefficient for a P wave to a P wave reflection.

There are several observations which can be made from Figs. 4 (a) and 4 (b). In Test I, although there are many possible P and S wave multiple reflections, only the multiple reflections of the P waves (s=0) and of the P waves containing a single S wave (s=1) are above the noise level. Most of these reflections are not overlapped significantly. This nonoverlapping case exists because the thickness of the plate is sufficiently large that the difference between the time delays for the successive significant reflections is adequately large. Thus the short- time Fourier analysis is suitable for

obtaining spectral information on individual reflections in the SWF signal shown in Fig. 4 (a).

In the SWF signal for Test II shown in Fig. 4 (b), successive reflections are overlapped and thus cannot be identified separately. This is because the thickness of the plate is so small that the difference between the time delays of the successive significant reflections is smaller than the length of a single reflection. Here, the short- time Fourier analysis does not give a direct access to spectral information. However, as discussed in Sec. 4, the short- time homomorphic analysis gives an estimate of the magnitude spectrum of a single reflection although it is overlapped with other adjacent (and perhaps beyond) reflections.

The short- time Fourier analysis of the SWF signal for Test I is obtained and spectral information on the reflection with p=12, s=0 is shown in Fig. 5. The time history of the short- time SWF signal, which is the reflection with p=12, s=0, and its log spectrum are shown in Figs. 5 (a) and 5 (b), respectively. The characteristics of the data window are indicated in the title for Fig. 5 (a). The origin of the abscissa (time) in Fig. 5 (a) is shifted to the beginning of the data window.

The short- time homomorphic analysis of the SWF signal for Test II is shown in Fig. 6. Here the goal is to obtain spectral information on the reflection with p=24, s=0. The process in Fig. 1, which is discussed in Sec. 4, is used. The short- time SWF signal and its log spectrum, cepstrum and cepstrally smoothed log spectrum are shown in Figs. 6 (a), (b), (c), and (d), respectively. Considering the discussions in Sec. 3, a Hamming window is used as the data window, and its beginning and end are chosen such that it covers the reflection with p=24, s=0 in its middle part. Since there is a compromise

in selecting the length of the window to satisfy the conditions for eqns. (5) and (6) simultaneously, the length of the data window is chosen by trial.

The log spectrum in Fig. 6 (a) contains rapid variations superposed onto what appears to be a slowly varying component. As discussed in Sec. 4, the rapid variations come from the impulse train which contains impulses located at the delays of the reflections in the short- time SWF signal.

Notice that the cepstrum in Fig. 6 (c) is substantially confined near zero. It also contains small peaks at ± 3.8 μsec away from zero. As discussed in Sec. 4, the small peaks away from zero are due to the impulse train and 3.8 μsec is approximately the same as the difference between the time delays of the reflections with only P waves.

The cepstrum in Fig. 6 (c) is multiplied by a Hamming window having a duration from -1.25 μsec to 1.25 μsec, which is called the cepstrum window, and then its FFT is taken to obtain the smoothed log spectrum in Fig. 6 (d). The Hamming window is chosen by trial. Considering the discussions in Sec. 4, its half length, 1.25 μsec, is chosen approximately one third of the length of the reflection with p=12, s=0 in Test I. The cepstrally smoothed log spectrum in Fig. 6 (d) is an estimate of the log spectrum of the reflection with p=24, s=0 in Test II. The log spectrum in Fig. 6(b) and the cepstrally smoothed log spectrum in Fig. 6 (d) are superposed in Fig. 6(e).

The short- time Fourier analysis of the SWF signal for Test I is repeated with different data windows to obtain log spectra of the reflections with p=8, s=0; and with p=10, s=0. Also, the short- time homomorphic analysis of the SWF signal in Test II is repeated with different data windows to obtain estimates to the log spectra of the reflections with p=16, s=0; and with p=20, s=0.

The characteristics of the log spectra of all the reflections considered above are listed in Table 2. The characteristics of the data windows are also indicated. The parameters used in Table 2 such as the peak log magnitude, peak frequency, average resonant frequency, lower and upper frequencies of -3 dB and -6 dB frequency bands are defined in Fig. 7 on a hypothetical log spectrum.

As discussed at the beginning of this section, since the reflection with $p=p_1$, $s=0$ in Test I and the reflection with $p=2p_1$, $s=0$ in Test II have the same ray angles, their log spectra are expected to have the same shapes but different scales. The characteristics of these two corresponding reflections are compared in Table 2 with the relative errors given in parentheses. The definition of the relative error is given in the Table 2 footnotes.

Notice that the -3 dB and the -6 dB frequency bands of the reflections in Tests I and II tend to move to higher frequencies for increasing values of p. As discussed in Sec. 3, this is because the reflections with larger values of p have smaller ray angles and the higher frequency components of the input signal are transmitted to the receiving transducer at smaller ray angles according to the directivity functions discussed in [10] and [11].

The discussions at the beginning of this section also suggest that the reflection with $p=2p_1$, $s=0$ in Test II is expected to be $(Q_{PP})^p$ times smaller than the reflection with $p=p_1$, $s=0$ in Test I. The values of $20 \log(Q_{PP})^p$ are read from Table 2 as the differences between the peak log magnitudes of the corresponding reflections in Tests II and I. Then, an experimental reflection coefficient for P waves to P waves is calculated for each value of p_1 considered.

The experimental reflection coefficients are compared with the

theoretical reflection coefficients in Table 3. The theoretical reflection coefficients are calculated from the formulae given in [10] and [23] for the reflection of plane P waves at a stress- free plane boundary. The incidence angle used in the formula is the same as the ray angle given in Table 1 for each value of p_1 considered. Notice that the experimental reflection coefficients are smaller than the corresponding theoretical reflection coefficients. This is consistent with the expectation that there is likely to be an energy loss (apart from mode conversions) in reflections.

Finally, two more tests are considered to demonstrate how the short-time homomorphic analysis given in this study may be utilized in the NDE of plates containing cracks perpendicular to its surfaces. For Test III ,the plate is the same as for Test II (h=1.25 cm, aluminum) and ℓ is 6 cm. For Test IV, the same plate, but now containing a crack, is used, and ℓ is again 6 cm. The crack is open to the bottom face of the plate like a slit all the way along the depth (into the plane of the sketch) of the plate. It has a depth d of 0.62 cm and a width of 0.05 cm. The crack faces are perpendicular to the crack and is located midway between the transducers.

The SWF signals for Tests III and IV are shown in Figs. 8 (a) and 8 (b), respectively. The time history of the short- time SWF signals, their log spectra and their cepstrally smoothed log spectra are shown in Figs. 9 (a) and 9 (b) for Tests III and IV, respectively. Considering the location of the data window, the cepstrally smoothed log spectra represent the estimates of the log spectra of the reflections with p=18, s=0 in both Tests III and IV. These two log spectra are compared in Table 4. The relative differences between the defined characteristics of the two log spectra are given in parentheses. The relative difference is defined under the Table 4 footnotes. No significant

relative differences in these defined characteristics are observed as indicators of the crack. However, the peak log magnitudes in Tests III and IV are -1.03 and -8.55, respectively. So, the peak log magnitude drops 7.52 dB (the peak magnitude drops to 42%) due to the existence of the crack.

5 CONCLUSIONS AND RECOMMENDATIONS

The SWF output signal was analyzed in the frequency domain. The SWF signal, which is the superposition of successive multiple reflections, was multiplied by a data window and its short- time portions were analyzed to obtain spectral information contained in individual reflections.

If the significant reflections were not overlapped, the short- time Fourier analysis was used; that is, the short- time SWF signal contained only a single reflection and its FFT was computed.

If the reflections were overlapped, it was assumed that the reflections in the short- time SWF signal have approximately the same waveform but different scales. This assumption suggested a data window which was tapered smoothly to zero at the beginning and the end of the window and long enough to cover the included reflections completely, but not so long that the waveforms of the included reflections changed significantly. Then, the short- time SWF signal was modelled as the convolution of an impulse train, where the impulses were located at the time delays of the reflections, and the reflection with the maximum scale.

A summary of the relevant points of homomorphic signal processing was given. Homomorphic signal processing was applied to short- time SWF signals to obtain estimates of the log spectra of individual reflections although the individual reflections were overlapped.

Two typical SWF signals generated in aluminum plates were analyzed. In Test I, the SWF signal contained nonoverlapping reflections. In Test II, the thickness of the plate was approximately half of that in Test I, and the reflections were overlapped. The reflection which was generated from the

stress waves which travelled p times as a P wave and s times as an S wave through the plate while reflecting back and forth between the bottom and top faces of the plate was designated as the reflection with p,s. The multiply reflected rays which were constructed geometrically between the centers of the transmitting and receiving transducers using Snell's law were considered. The distances between the transducer axes in Tests I and II were chosen such that the reflections with $p=p_1$, $s=0$ in Test I and the reflections with $p=2p_1$, $s=0$ in Test II had the same ray angles and approximately the same total ray path lengths. The theoretical analysis suggested that the magnitude spectra of the two corresponding reflections with the same ray angles in Tests I and II were expected to have the same shape but different scales because all the frequency components of the input signal are transmitted to the reflections from the same directions.

The log spectra of the reflections with $p=p_1$, $s=0$ in Test I were obtained by the short- time Fourier analysis for the values of p_1 of 8, 10, and 12. The estimates of the log spectra of the corresponding reflections with $p=2p_1$, $s=0$ in Test II were obtained by the short- time homomorphic analysis. The characteristics of the log spectra of the two corresponding reflections in Tests I and II were compared in terms of their peak log magnitudes, peak frequencies, average resonant frequencies, and lower and upper frequencies of -3 dB and -6 dB frequency bands. It was observed that in general they were approximately the same except for the peak log magnitudes, as the theory of wave propogation in isotropic elastic plates suggested.

From the differences between the peak log magnitudes and between the values of p in Tests I and II, experimental reflection coefficients were calculated for different ray angles. These showed good agreement with the

theoretical reflection coefficients for plane waves. Also, it was observed that frequency bands of the reflections with larger p, namely with smaller ray angles, moved to higher frequencies, which was consistent with the behavior of the directivity function of the P wave.

Finally, the potential use of the results of this study for the NDE of plates containing cracks perpendicular to their faces was demonstrated in a specific test. For a specific set of parameters such as the input signal, plate thickness, crack depth, location, and orientation, it was observed that the decrease in the peak log magnitude of a specific reflection, which was found by the short- time homomorphic analysis, was the indicator of the crack.

This study provides a quantitative analysis of the SWF signal in the frequency domain. Since the information in the frequency domain can be related directly to the steady- state wave propagation analysis in test structures, it should provide more revealing measurements for NDE applications utilizing the SWF. The effect of different cracks on the characteristics of the log spectra of different reflections should be analyzed. This study may be useful in the analysis of the ultrasonic output signals in different test structures which may contain overlapped reflections. Ultrasonic attenuation measurements and transducer calibration techniques may benefit from this study. The short- time homomorphic analysis may also be applied to acoustic emission (AE) signals to characterize unknown sources in terms of their directivity functions. Finally, developments in CANDE should be faciliated by the digital signal processing procedures which are summarized in this study.

REFERENCES

[1] A.V. Oppenheim, A.S. Willsky, with I.T. Young, Signals and Systems, Prentice- Hall, Inc., Englewood Cliffs, N.J., 1983.

[2] J.W. Cooley and J.W. Tukey, "An Algorithm for the Machine Computation of Compex Fourier Series', Mathematics of Computation, Vol. 19, No. 89, April 1965, pp. 297- 301.

[3] A.V. Oppenheim, R.W. Schafer, Digital Signal Processing, Prentice-Hall, Inc., Englewood Cliffs, N.J., 1975.

[4] J. Krautkramer and H. Krautkramer, Ultrasonic Testing of Materials, Second Edition, Springer- Verlag, N.Y., 1977.

[5] D.W. Fitting and L. Adler, Ultrasonic Spectral Analysis for Nondestructive Evaluation, Plenum Press, N.Y., 1981.

[6] A. Vary and R.F. Lark, "Correlation of Fiber Composite Tensile Strength with the Ultrasonic Stress Wave Factor", Journal of Testing and Evaluation, Vol. 7, No. 4, July 1979, pp. 185- 191.

[7] A. Vary and K.J. Bowles, "An Ultrasonic- Acoustic Technique for Nondestructive Evaluation of Fiber Composite Quality", Polymer Engineering and Science, Vol. 19, No. 5, April 1979, pp. 373- 376.

[8] J.H. Williams, Jr. and N.R. Lampert, "Ultrasonic Evaluation of Impact-Damaged Graphite-Fiber Composite", Materials Evaluation, Vol. 38, No. 12, December 1980, pp. 68-72.

[9] R.H. Wehrenberg II, "New NDE Technique Finds Subtle Defects", Materials Engineering, Vol. 92, No. 3, September 1980, pp. 59-63.

[10] J.H. Williams, Jr., H. Karagulle, and S.S. Lee, "Ultrasonic Input-Output for Transmitting and Receiving Longitudinal Transducers Coupled to Same Face of Isotropic Elastic Plate", Materials Evaluation, Vol. 40, No. 6, May 1982, pp. 655-662.

[11] H. Karagulle, J.H. Williams, Jr., S.S. Lee, "Stress Waves in an Isotropic Elastic Plate Excited by a Circular Transducer", Composite Materials and Nondestructive Laboratory, Massachusetts Institute of Technology, Cambridge, Mass., Unpublished Report, 1984.

[12] H. Karagulle, S.S. Lee, and J.H. Williams, Jr., "Input-Output Characterization of Ultrasonic Testing System by Digital Signal Analysis", Report no. CR-3756, National Aeronautics and Space Administration, Washington, D.C., January 1984.

[13] L.R. Rabiner and R.W. Schafer, Digital Processing of Speech Signals, Prentice-Hall, Inc., Englewood Cliffs, N.J., 1978.

[14] R.W. Schafer, "Echo Removal by Discrete Generalized Linear Filtering", Technical Report no. 466, Research Laboratory of Electronics, Massachusetts Institute of Technology, Cambridge, Mass., February 1969.

[15] A.V. Oppenheim, "Superposition in a Class of Nonlinear Systems", Technical Report no. 432, Research Laboratory of Electronics, Massachusetts Institute of Technology, Cambridge, Mass., March 1965.

[16] A.V. Oppenheim, R.W. Schafer, and T.G. Stockham, Jr., "Nonlinear Filtering of Multiplied and Convolved Signals", Proceedings of the Institute of Electrical and Electronics Engineers, Vol. 56, No. 8, August 1968, pp. 1264- 1291.

[17] A.V. Oppenheim and R.W. Schafer, "Homomorphic Analysis of Speech", The Institute of Electrical and Electronics Engineers Transactions on Audio and Electroacoustics, Vol. AU-16, No.2, June 1968, pp. 221- 226.

[18] A.V. Oppenheim, "Speech Analysis- Synthesis System Based on Homomorphic Filtering", The Journal of the Acoustical Society of America, Vol. 45, No. 2, February 1969, pp. 458-465.

[19] R.W. Schafer and L.R. Rabiner, "System for Automatic Formant Analysis of Voiced Speech", The Journal of the Acoustical Society of America, Vol. 47, No. 2 (Part 2), February 1970., pp. 634- 648.

[20] T.J. Ulrych, "Application of Homomorphic Deconvolution to Seismology",

Geophysics, Vol. 36, No. 4, August 1971, pp. 650- 660.

[21] A.V. Oppenheim, "Digital Processing of Speech", Application of Digital Signal Processing, Ed. by A.V. Oppenheim, Prentice- Hall, Englewood Cliffs, N.J., 1978, pp. 117- 168.

[22] B.P. Bogert, M.J.R. Healy, and J.W. Tukey, "The Quefrency Alanysis of Time Series for Echoes: Cepstrum, Pseudo- Autocovariance, Cross- Cepstrum, and Saphe Cracking", Symposium on Time Series Analysis, Proceedings, Brown University, 1962, sponsored jointly by the Office of Naval Research and Brown University, Ed. by M. Rosenblatt, John Wiley & Sons, Inc., N.Y., 1963, pp. 209- 243.

[23] K.F. Graff, Wave Motion in Elastic Solids, The Ohio State University Press, Columbus, OH, 1975.

TABLE 1 Ray Angles, Total Ray Path Lengths, and Time Delays for Some Reflections With Only P waves in Tests I and II.

Test	p	Ray Angle (Degree)	Total Ray Path Length (cm)	Time Delay (μsec)
I	8	17.35	20.12	31.83
	10	14.04	24.74	39 14
	12	11.77	29 42	46.55
II	16	17.35	20.95	33.15
	20	14.04	25.77	40 77
	24	11.77	30.64	48.49

TABLE 2 Characteristics of Log Spectra of Some Reflections With Only P Waves in Tests I and II

Test	p	Method of Analysis	Data Window		Peak Log Magnitude (dB)	Peak Frequency (MHz)	Average Resonant Frequency (MHz)	Frequency Bands (MHz)			
								-3 dB		-6 dB	
			Type	Interval (μsec)				Lower Frequency	Upper Frequency	Lower Frequency	Upper Frequency
I	8	STF[a]	Rectangular	31.8 to 35.3	10.07	0.82	1	0.61	1.39	0.54	1.64
	10	STF	Rectangular	39.1 to 42.6	10.04	1.05	1.19	0.82	1.55	0.74	1.71
	12	STF	Rectangular	46.5 to 50	8.42	1.48	1.49	1.07	1.90	0.95	2.09
II	16	STH[b]	Hamming	24.7 to 42.7	-1.70	1.02 (24 %)[c]	1.17 (17 %)	0.65 (7 %)	1.69 (22 %)	0.54 (0 %)	1.95 (19 %)
	20	STH	Hamming	32.3 to 50.3	-0.03	1.33 (27 %)	1.3 (9 %)	0.88 (7 %)	1.72 (11 %)	0.66 (11 %)	1.90 (11 %)
	24	STH	Hamming	39.9 to 50.3	-2.01	1.56 (5 %)	1.44 (3 %)	0.95 (11 %)	1.93 (2 %)	0.69 (27 %)	2.10 (0.5 %)

a STF Short-time Fourier analysis

b STH Short-time homomorphic analysis

c The values in the parentheses show the relative error, e_r, between the value above the parenthesis for the reflection with $2p_1$, s=0 in Test II, V_{II}, and the corresponding value for the reflection with $p=p_1$, s=0 in Test I, V_I, such that $e_r=|V_{II}-V_I|/V_I$ (p_1=8, 10, 12).

ORIGINAL PAGE IS OF POOR QUALITY

TABLE 3 Comparison of Experimental and Theoretical Reflection Coefficients.

Value of p		Ray Angle (Degree)	Theoretical Reflection Coefficient[a] $(Q_{PP})_t$	Experimental Reflection Coefficient $(Q_{PP})_e$	Relative Error[b] (%)
Test I	Test II				
8	16	17.35	0.915	0.844	7.8
10	20	14.04	0.943	0.890	5.6
12	24	11.77	0.960	0.905	5.7

a Absolute values are given.

b Relative Error = $|(Q_{PP})_t - (Q_{PP})_e| / |(Q_{PP})_t|$

TABLE 4 Characteristics of Log Spectra of Reflections With p=18, s=0 in Tests III and IV

Test	p	Method of Analysis	Data Window		Peak Log Magnitude (dB)	Peak Frequency (MHz)	Average Resonant Frequency (MHz)	Frequency Bands (MHz)			
			Type	Interval (μsec)				-3 dB		-6 dB	
								Lower Frequency	Upper Frequency	Lower Frequency	Upper Frequency
III	18	STH[a]	Hamming	28.45 to 46.45	-1.03	1.45	1.38	0.95	1.81	0.74	1.97
IV	18	STH	Hamming	28.45 to 46.45	-8.55	1.37 (6 %)[b]	1.29 (7 %)	0.76 (20 %)	1.81 (0 %)	0.60 (19 %)	2.00 (2 %)

a STH Short-time homomorphic analysis

b The values in the parentheses show the relative difference, d_r, between the value above the parenthesis for the reflection in Test IV, V_{IV}, and the corresponding value for the reflection in Test III, V_{III}, such that

$$d_r = |V_{IV} - V_{III}| / V_{III}$$

ORIGINAL PAGE IS
OF POOR QUALITY

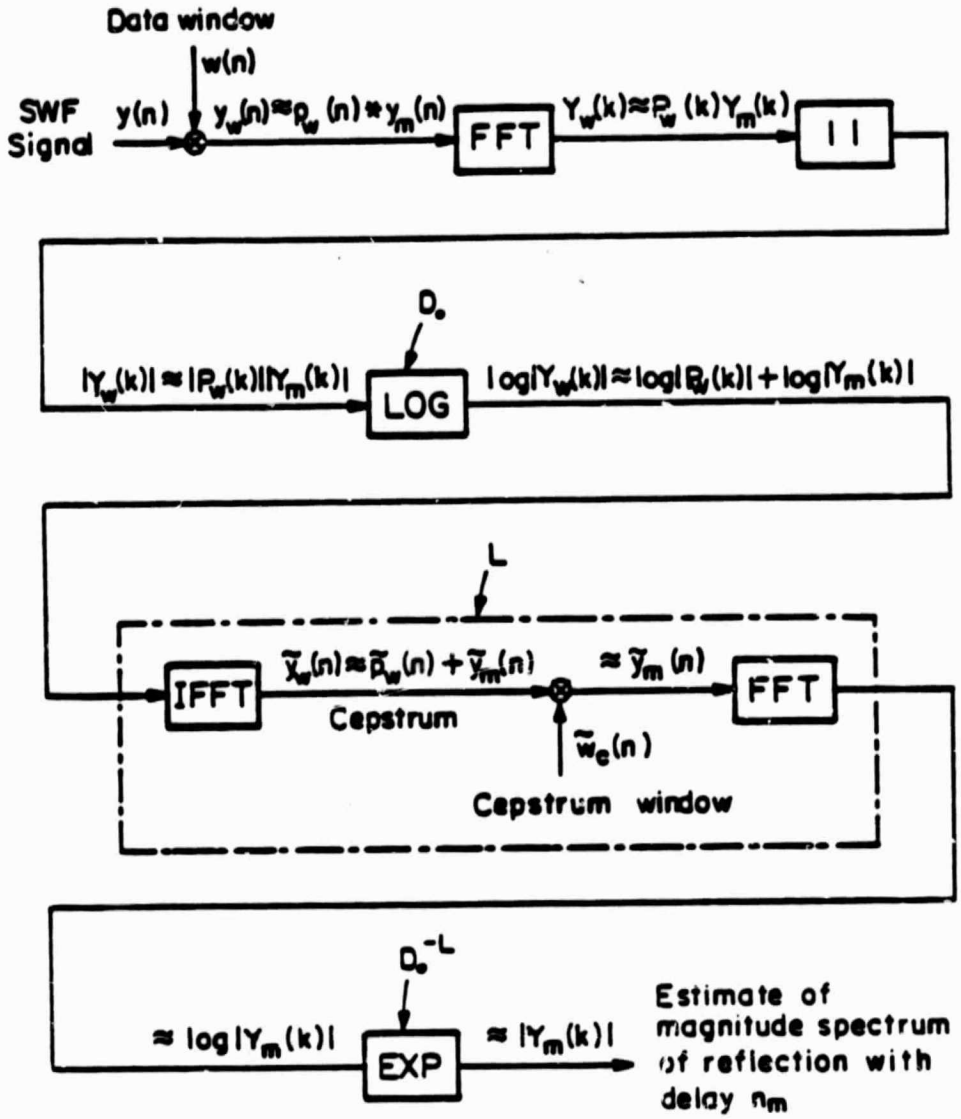

Fig. 1 Schematic of homomorphic signal processing of SWF output signal to estimate magnitude spectrum of a particular reflection.

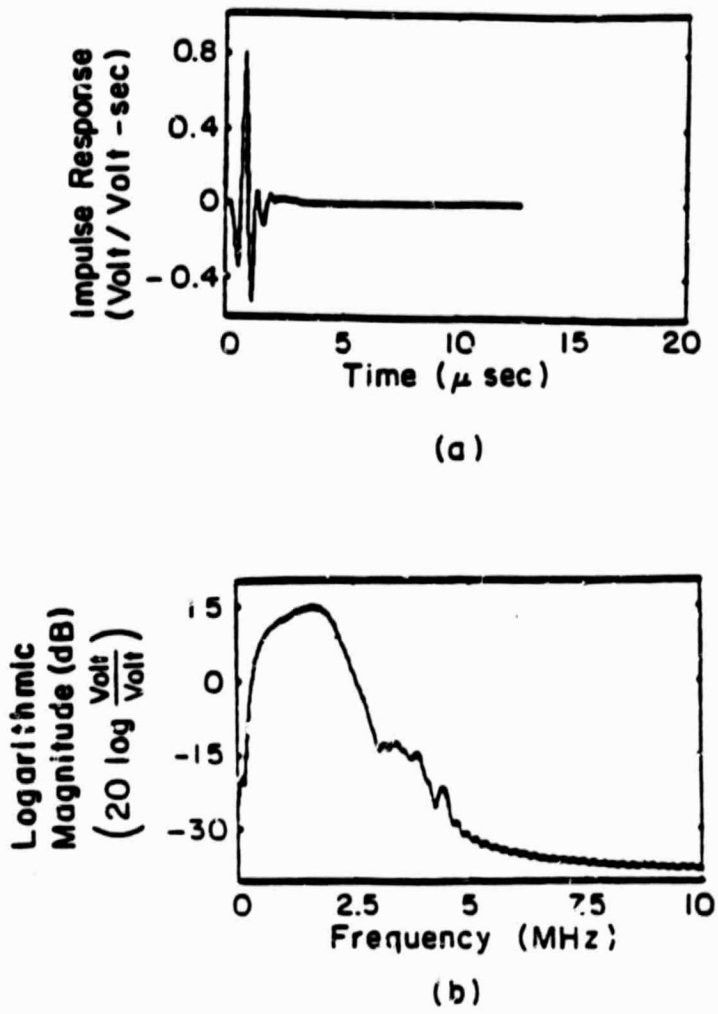

Fig. 2 Experimental system characteristics (a) impulse response and (b) log spectrum (peak at 1.7 MHz with 14.66 dB, -3 dB frequency band 0.9 to 2.1 MHz, -6 dB frequency band 0.6 to 2.3 MHz).

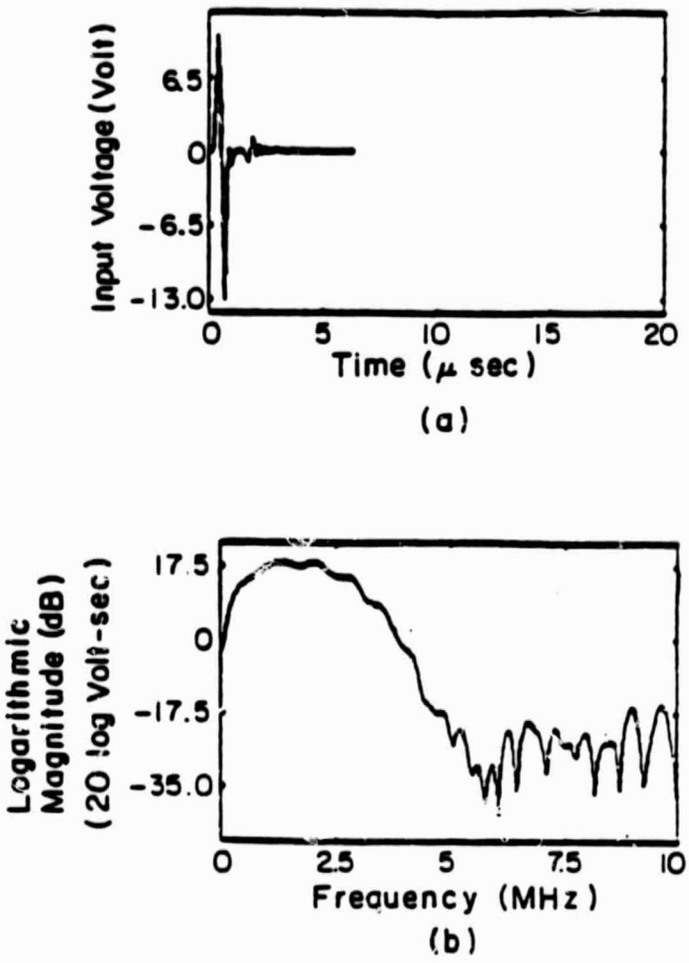

Fig 3 Input signal (a) time history and (b) log spectrum (peak at 1.25 MHz with 35.7 dB. -3 dB frequency band 0.8 to 2.4 MHz. -6 dB frequency band 0.4 to 3 MHz)

ORIGINAL PAGE IS
OF POOR QUALITY

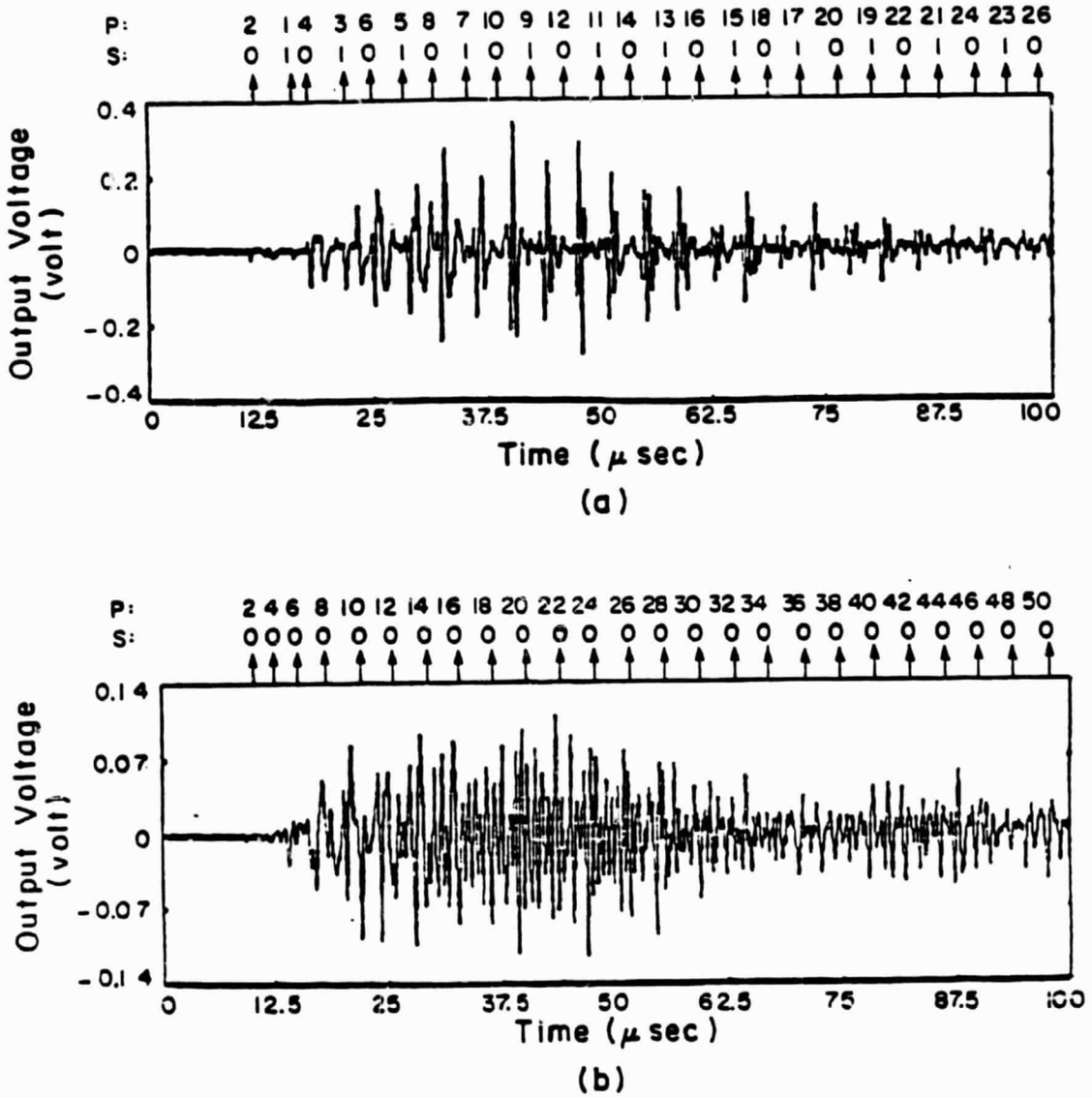

Fig. 4 Time history of SWF output signals for (a) Test I (h=2.4 cm, ℓ=6 cm) and (b) Test II (h=1.25 cm, ℓ=6.25 cm).

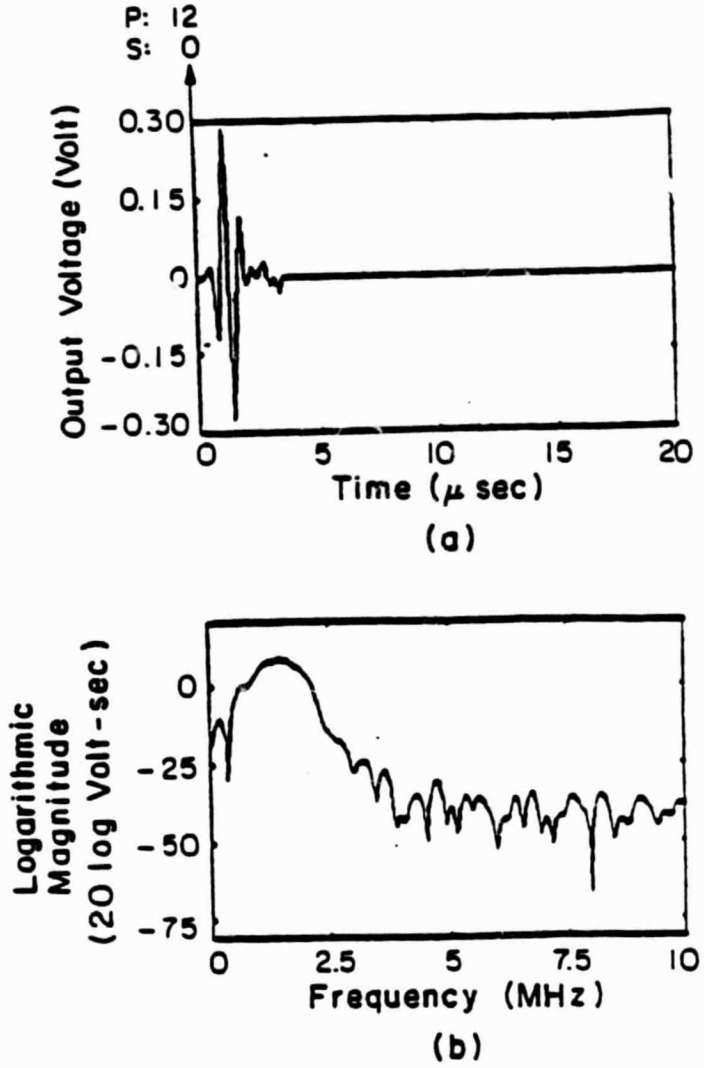

Fig. 5 Short-time Fourier analysis of SWF output signal for Test I (a) time history (data window: rectangular, 46.5 to 50 μsec) and (b) log spectrum.

ORIGINAL PAGE IS
OF POOR QUALITY

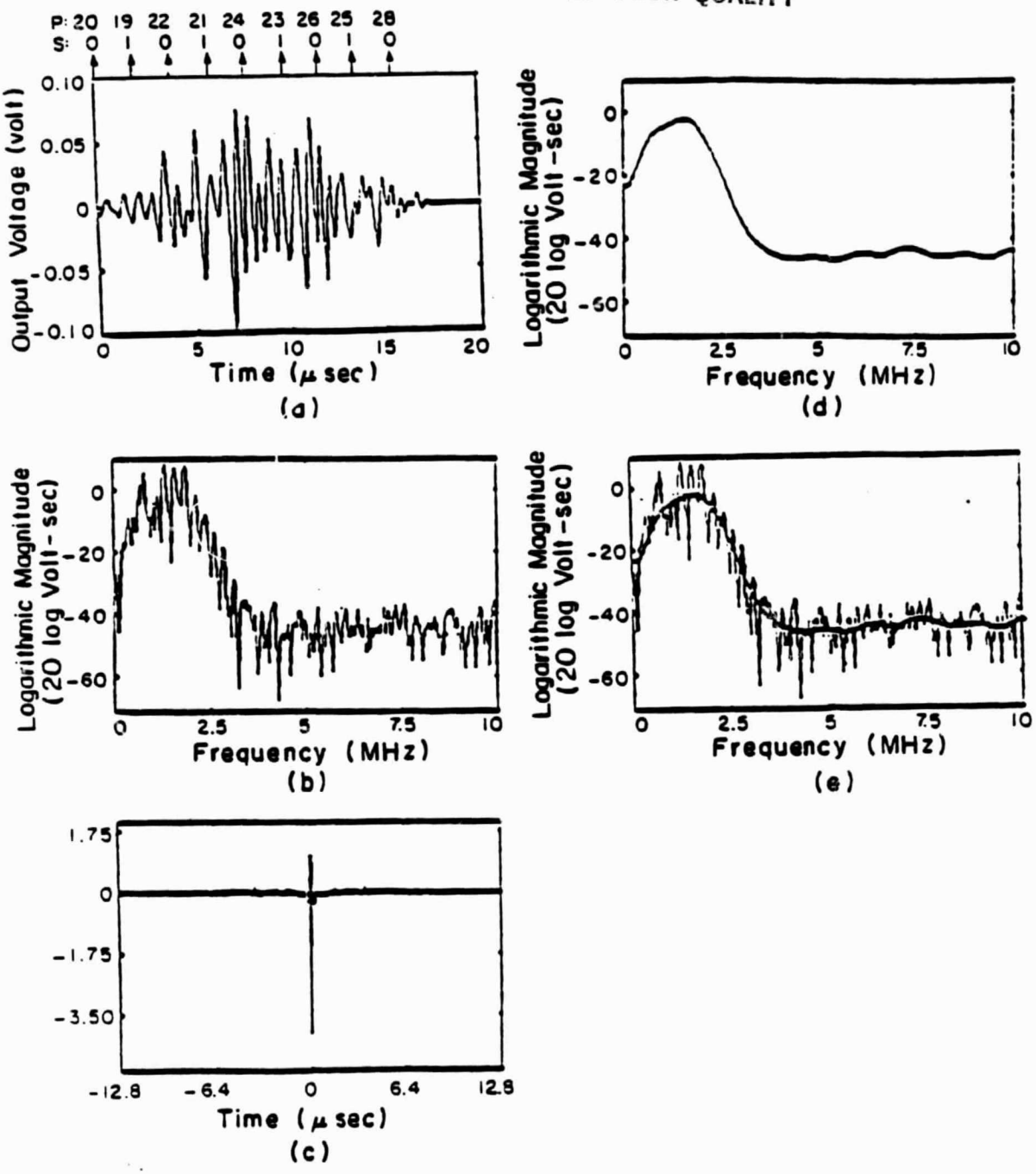

Fig. 4 Short-time homomorphic analysis of SWF output signal for Test II (a) time history (data window: Hamming, 39.9 to 57.9 μsec), (b) log spectrum, (c) cepstrum, (d) cepstrally smoothed log spectrum , and (e) superposition of (b) and (d).

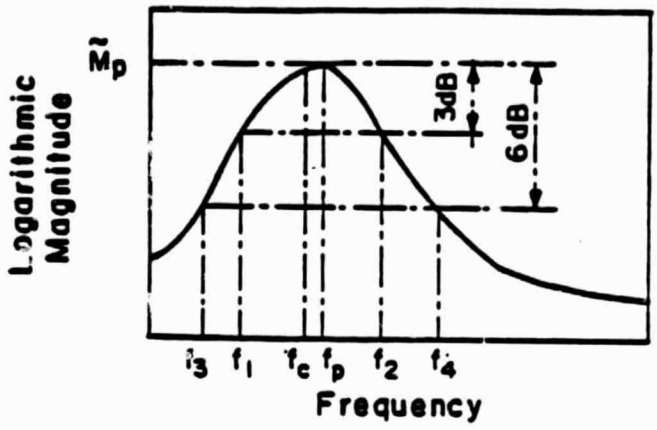

f_p	: Peak frequency
f_1	: Lower frequency of -3 dB frequency band
f_2	: Upper frequency of -3 dB frequency band
f_3	: Lower frequency of -6 dB frequency band
f_4	: Upper frequency of -6 dB frequency band
$f_c=(f_1+f_2)/2$	: Average resonant frequency
$\tilde{M}_p$	: Peak log magnitude

Fig. 7 Definitions of parameters on hypothetical log spectrum.

ORIGINAL PAGE IS
OF POOR QUALITY

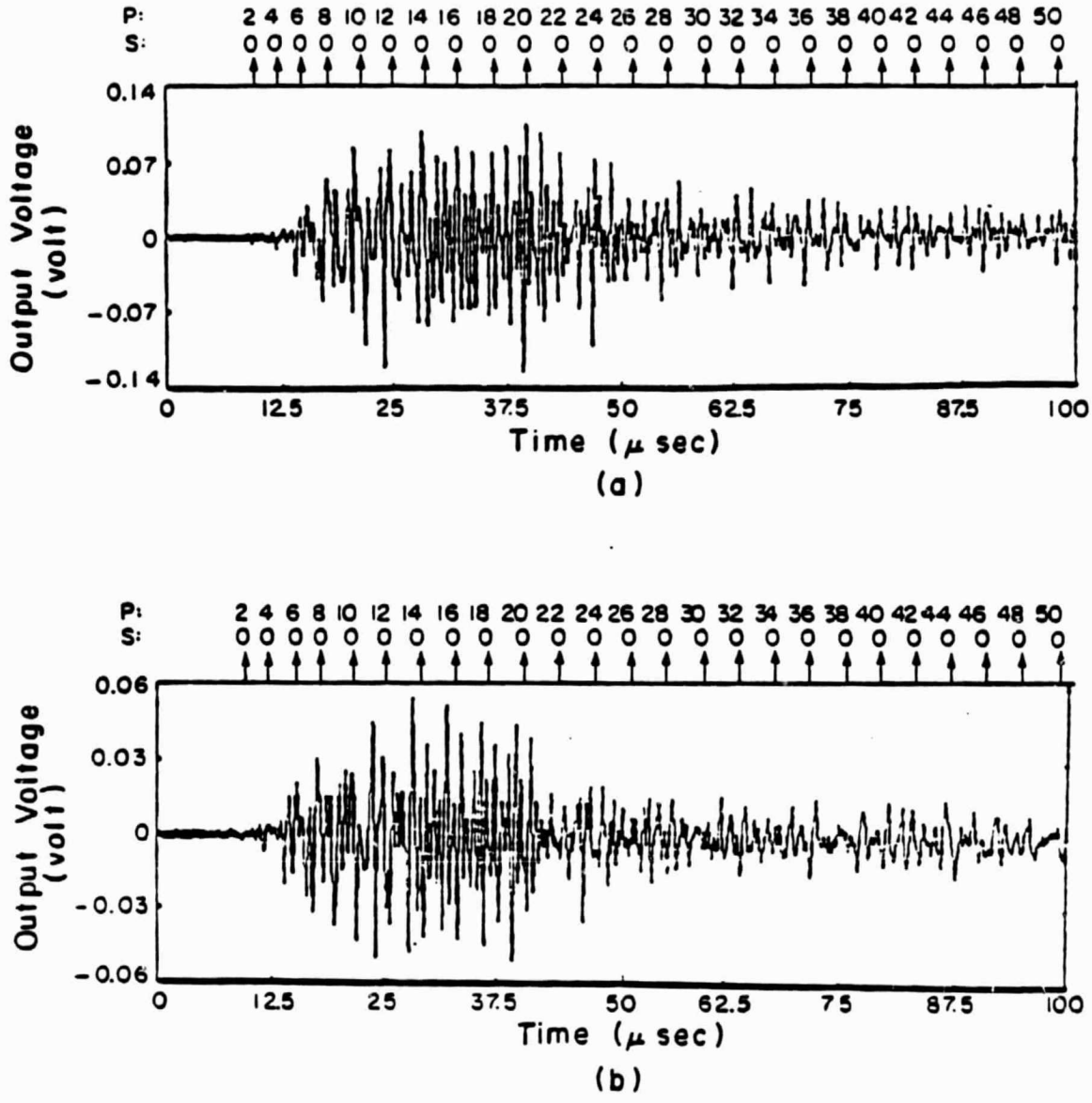

Fig. 8 Time history of SWF output signal for (a) Test III (h=1.25 cm, ℓ=6 cm, d=0), and (b) Test IV (h=1.25 cm, ℓ=6 cm, d=0.62 cm).

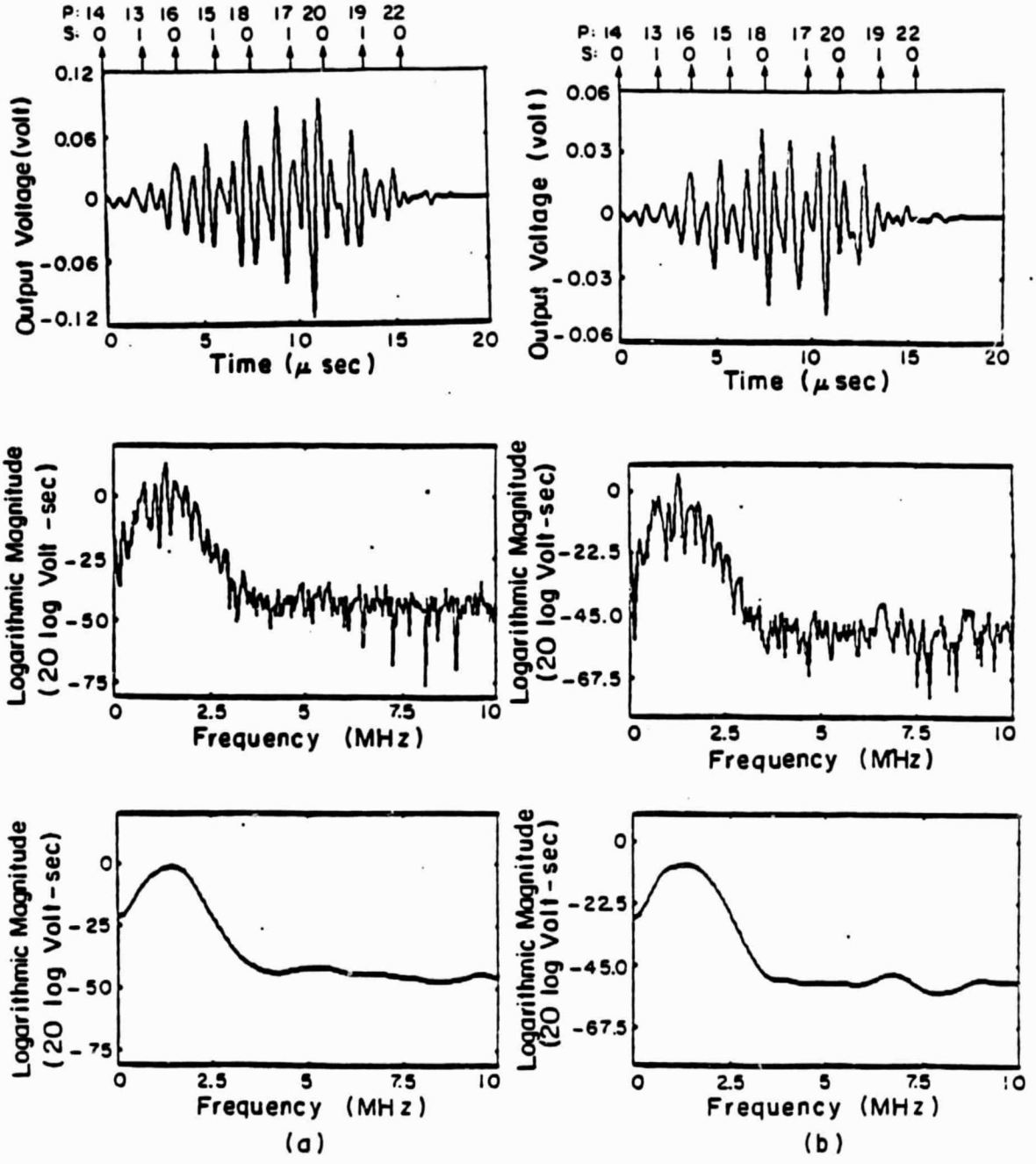

Fig. 9 Time history, log spectrum, and cepstrally smoothed log spectrum in short-time homomorphic analysis of TWF output signals for (a) Test III and (b) Test IV.

1. Report No.	2. Government Accession No.	3. Recipient's Catalog No.
NASA CR-174871		

4. Title and Subtitle	5. Report Date
Application of Homomorphic Signal Processing to Stress Wave Factor Analysis	February 1985
	6. Performing Organization Code

7. Author(s)	8. Performing Organization Report No.
Hira Karagulle, James H. Williams, Jr., and Samson S. Lee	None
	10. Work Unit No.

9. Performing Organization Name and Address	11. Contract or Grant No.
Massachusetts Institute of Technology Dept. of Mechanical Engineering Cambridge, Massachusetts 02139	NSG 3-328
	13. Type of Report and Period Covered
12. Sponsoring Agency Name and Address	Contractor Report
National Aeronautics and Space Administration Washington, D.C. 20546	14. Sponsoring Agency Code
	506-53-1A

15. Supplementary Notes

Final report. Project Manager, Alex Vary, Structures Division, NASA Lewis Research Center, Cleveland, Ohio 44135.

16. Abstract

The stress wave factor (SWF) signal, which is the output of an ultrasonic testing system, where the transmitting and receiving transducers are coupled to the same face of the test structure, is analyzed in the frequency domain. The SWF signal generated in an isotropic elastic plate is modelled as the superposition of successive reflections. The reflection which is generated by the stress waves which travel p times as a longitudinal (P) wave and s times as a shear (S) wave through the plate while reflecting back and forth between the bottom and top faces of the plate is designated as the reflection with p, s. Short-time portions of the SWF signal are considered for obtaining spectral information on individual reflections. If the significant reflections are not overlapped, the short-time Fourier analysis is used. A summary of the relevant points of homomorphic signal processing, which is also called cepstrum analysis, is given. Homomorphic signal processing is applied to short-time SWF signals to obtain estimates of the log spectra of individual reflections for cases in which the reflections are overlapped. Two typical SWF signals generated in aluminum plates are analyzed. In Test I, the SWF signal contains nonoverlapping reflections. In Test II, the thickness of the plate is approximately half that in Test I, and the reflections are overlapped. Multiple reflections of only P waves are considered. It is observed that the log spectra of two corresponding reflections with the same ray angles and approximately the same total ray path lengths in Tests I and II have approximately the same characteristics except for their overall scales, as the theory of wave propagation in isotropic elastic plates suggests. From the differences between the overall scales and the values of p of the two corresponding reflections in Tests I and II, experimental reflection coefficients for P wave to P wave reflections are obtained for the different ray angles considered. They show good agreement with the theoretical reflection coefficients for plane P waves. Also, it is observed that the frequency response at the maximum value of the log spectrum moves toward higher frequencies in the reflections with larger p, namely with smaller ray angles. This is consistent with the behavior of the directivity function. The potential use of these results for the nondestructive evaluation of plates containing cracks perpendicular to their faces is demonstrated in a specific test.

17. Key Words (Suggested by Author(s))	18. Distribution Statement
Nondestructive testing; Ultrasonics; Acousto-ultrasonics; Stress waves; Signal analysis; Longitudinal and shear waves; Fourier Transform Analysis	Unclassified - unlimited STAR Category 38

19. Security Classif. (of this report)	20. Security Classif. (of this page)	21. No. of pages	22. Price*
Unclassified	Unclassified	47	A03

*For sale by the National Technical Information Service, Springfield, Virginia 22161